Physics and applications of ICRH on W7-X

J.Ongena[1], Ye.O.Kazakov[1], B.Schweer[1], F.Louche[1], A.Messiaen[1], M.Vervier[1], V.Borsuk[2,3], R. Bilato[5], D.A.Hartmann[3], K-P.Hollfeld[5], J.P. Kallmeyer[3], A.Krivska[1], O.Neubauer[2], D. Van Eester[1], M. Van Schoor[1], T.Wauters[1], R.C.Wolf[43] and the W7-X team[3]

[1]Laboratory for Plasma Physics, Ecole Royale Militaire-Koninklijke Militaire School, 1000 Brussels, Belgium, TEC Partner
[2]Institut für Energie- und Klimaforschung / Plasmaphysik (IEK-4), Forschungszentrum Jülich, D-52435 Jülich, Germany, TEC Partner
[3]Max-Planck-Institut für Plasmaphysik, Wendelsteinstraße 1, D-17491 Greifswald, Germany
[4]Max-Planck-Institut für Plasmaphysik, Boltzmannstraße 2, D-85748 Garching bei München, Germany
[5]Zentralinstitut für Engineering, Elektronik und Analytik –Engineering und Technologie, (ZEA-1), Forschungszentrum Jülich, D-52425 Jülich, Germany

E-mail contact of main author: j.ongena@fz-juelich.de

Abstract. An important aim of W7-X is to demonstrate fast ion confinement at volume averaged beta values up to 5%, corresponding to plasma densities above 10^{20} m^{-3}. To this end, an ICRH system is prepared for W7-X, with RF power up to ~1.5 MW (depending on the coupling) at frequencies between 25-38 MHz in pulses up to 10 s. For optimal coupling the antenna surface is carefully matched to the standard magnetic configuration of W7-X. Gas puffing is foreseen to optimize coupling to other magnetic scenarios. To measure the density profile in front of the antenna and for edge plasma turbulence studies, an installation of the microwave reflectometer system is provisionally foreseen at a later stage.
Energetic ions in W7-X with energies 50 < E < 100 keV mimic alphas in a reactor. To generate such population is challenging in high density plasmas. The production of fast particles is rather efficient using a new so-called three-ion heating ICRH scenario. Two majority gases (e.g. H and ^{4}He / H and D) are used in a well chosen proportion to locate the maximum of the left-hand polarized electric field (E+) of the magnetosonic wave at the resonance position of a third minority species (^{3}He). This scheme allows using a low concentration of ^{3}He (< 1%), thus a large amount of RF power is absorbed per particle. In this way perpendicular energies between 50 and 100 keV or higher should be reached, even at plasma densities above 10^{20} m^{-3}. The three-ion scheme is foreseen for use at f ~ 25 MHz. At f ~ 38 MHz, also H minority heating or second harmonic ^{4}He / D majority absorption can be used, depending on the H minority concentration. In addition to all this, ICRH is also planned for Ion Cyclotron Wall Conditioning on W7-X.

1. Introduction

The stellarator Wendelstein 7-X (W7-X) that recently started operations in the Max-Planck Institute in Greifswald, is equipped with superconducting coils, allowing plasma pulses of up to 30 minutes duration. ECRH is the main heating system at power levels up to 10 MW at 140 GHz. In addition, up to 10 s pulses of neutral beam injection (stepwise upgrading from 3.5 to 20 MW) are foreseen to explore beta and stability limits. An important aim of W7-X is to demonstrate fast ion confinement at volume averaged beta values up to 5% [1]. The highest beta values correspond to plasma densities above 10^{20} m^{-3}.

Mimicking the behaviour of alpha particles in a future stellarator requires the presence of energetic ions in the core of W7-X plasmas with energies in the range 50-100 keV. Given the expected high plasma densities, this is a challenging task. As will be explained below, such a population can be created using Ion Cyclotron Resonance Heating (ICRH) using different

ICRH scenarios. The most important of them is the newly developed [2] and recently experimentally verified 3-ion heating scenario [3, 4], that uses a low concentration of a third ion, in a plasma consisting of a well determined mix of two main ions and should allow to create at densities above $10^{20}m^{-3}$ fast ions with energies required for the demonstration of equivalent fusion alpha confinement in a Helios reactor. The ICRH antenna can also be used for plasma heating, current drive, plasma startup and ICRH wall conditioning.

This paper describes the challenges in the mechanical and electromagnetic design of this antenna, and summarizes the physics applications of ICRH on W7-X.

2. Main design challenges for the ICRH Antenna for Wendelstein 7-X

An ICRH antenna consisting of two poloidal straps is now under construction for W7-X in a collaboration between the Institut für Energie und Klimaforschung/Plasmaphysik of the Forschungszentrum Jülich (IEK-4/FZJ) and the Laboratory for Plasma Physics of the Ecole Royale Militaire/Koninklijke Militaire School (LPP-ERM/KMS). Each strap is on one side connected to a tuning capacitor (2-200 pF) and grounded to the antenna box at the other end [5].

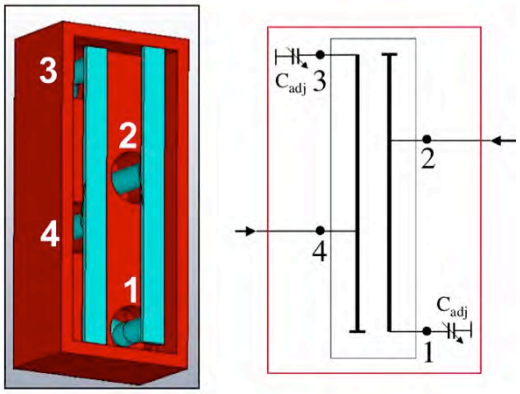

FIG. 1: Schematic view of the W7-X ICRH antenna and its equivalent circuit [5].

To reduce the voltage in the feeding transmission lines and matching system, a pre-matching has been implemented by connecting the RF transmission lines at an intermediate position on each strap (FIG. 1). The strap width, strap length and antenna box depth have been optimized to maximise the power delivered to the plasma, using the reference plasma density profile in front of the antenna, as provided by the W7-X team. Such an optimization was done with ANTITER, and later with the commercially available 3D electromagnetic code CST Microwave Studio (MWS) and the TOPICA code, which calculates the 4x4 scattering matrix of the antenna box (consisting of a 4 port network with the two capacitor ports and taps feeds) and using the reference plasma density profile as provided by the W7-X team in front of the antenna.

The calculations have been checked experimentally using a novel technique with $BaTiO_3$ as simulation for the plasma load [6]. To maximise coupling for a large fraction of the operational time, the shape of the two-strap ICRH antenna is carefully matched to the 3D shape of the Last Closed Magnetic Surface (LCMS) of the standard magnetic field configuration (m/n=5/5) in W7-X. Therefore the surface of the antenna requires a variable curvature in both toroidal and poloidal directions. This is the first time that an ICRH antenna with such a complex 3D shape is built, requiring state-of-the-art Computerized Numerical Control (CNC) mechanical construction equipment. To cope with other magnetic scenarios that have a different radial extension, the antenna can be moved radially over max. 35 cm and in order to locally improve the coupling for configurations with a different LCMS shape, a gas puffing system is integrated in the carbon antenna protection tiles to blow gas in the region between the scrape-off layer (SOL) and the LCMS. A test stand is currently under construction to check the mechanical, thermal, electromagnetic and vacuum properties of the

antenna system. It is envisaged to have the ICRH system ready for use in the operational phase 1.2b (OP1.2b) of W7-X.

3. Mechanical design

An overview of the full system, highlighting the main components, is presented in FIG. 2. The antenna head consists of a stainless steel box (outer dimensions: 924 mm height, 378 mm width), with two straps (866 mm height, 90 mm width, 15 mm thickness). To avoid short-circuiting of the straps to antenna box or plasma via the magnetic field lines, the straps are recessed inside the antenna box by 10 mm. The plasma facing surfaces of the antenna box are shielded with graphite tiles that are also shaped according to the LCMS of the standard magnetic configuration within ±0.3 mm accuracy. The heat load from the plasma is removed by cooling water channels underneath the tiles and near the rear side of the box.

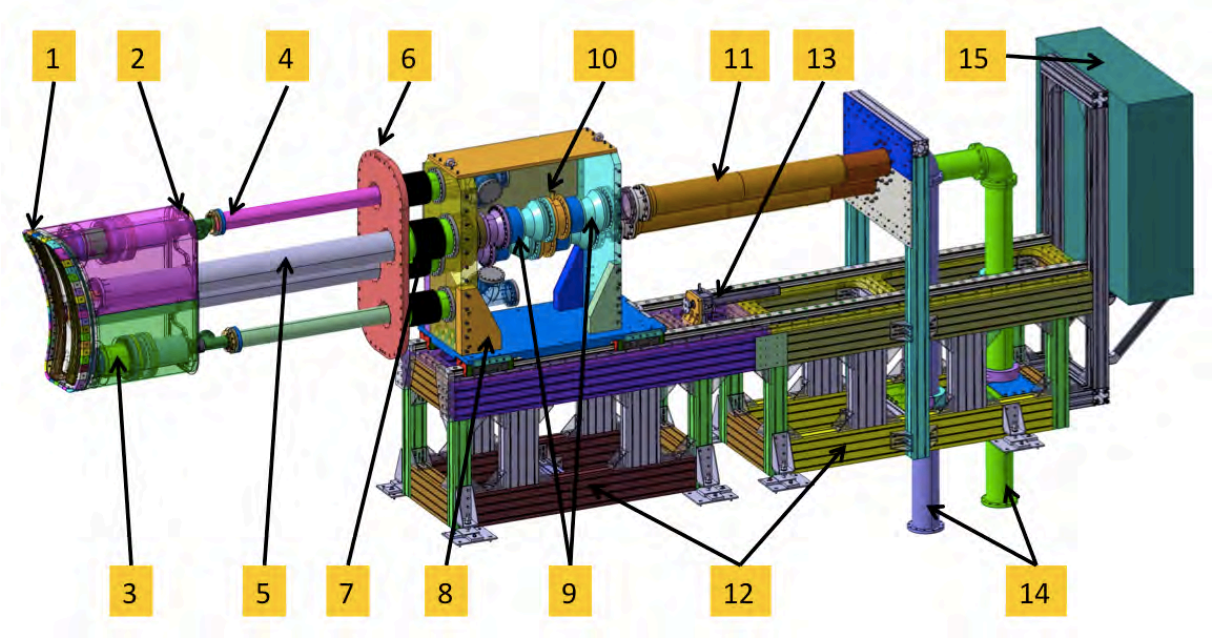

FIG. 2: Overview of the ICRH antenna system under construction for W7-X (1:antenna head with carbon protection tiles, 2:short circuit to AEE31 duct, 3:tunable capacitor, 4:supply tubes for water cooling circuits and diagnostics, 5:coaxial RF transmission line, 6:cryostat flange, 7:bellow, 8:movable antenna support, 9:RF feedthroughs, 10:vacuum control volume, 11:line stretcher, 12:support tables, 13:motor for radial motion of the antenna head assembly, 14:RF lines interface with DC break, 15:electrical cabinet with local control WinCC panel) [7]

When not in use, the antenna is retracted into its port duct (labelled AEE31 on W7-X). During operations the antenna can be moved radially over 350mm (with a speed of 3 mm/s) to come as close as possible near the LCFS of the magnetic configuration in use. This speed is sufficient to avoid a too large increase in temperature from plasma irradiation.

The temperature distribution in the cross-section of the graphite and stainless steel wall parts of the antenna head are modelled with ANSYS assuming a conductive heat exposure of 1.0 MW/m^2 at the tip of the graphite tiles, an exponential power decay length of 10 mm and a heat transfer coefficient in the graphite foil of 1 kW/(m^{2}K). At the graphite tile the surface temperature reaches up to 940^{o}C with a large temperature drop of about 550 K within the graphite foil. This has been confirmed experimentally with a mock-up irradiated with the

electron beam device JUDITH-1 [8]. Moreover, equilibrium surface temperatures of about 1500°C were obtained with repetitive heat load pulses of 2 MW/m^2 without any damage to the tiles.

The water-cooled straps are made of low cobalt stainless steel (SS1.4429, Co≤500ppm). The surface temperature is mainly influenced by CW irradiation from the W7-X plasma, which in the worst case (a detached plasma) can be up to 100 kW/m^2. During antenna operation the straps receive an additional heat load from the RF within the skin depth.

For the grounding of the antenna box air powered pistons are used to press electrical contacts to the duct. Using this system, the grounding is also guaranteed during movement of the antenna in the port duct. The RF transmission lines mechanically carry the weight the antenna box and are connected with a radially movable carrier (Pos. 8, FIG.2) outside the cryostat. UHV conditions are maintained by edge-welded bellows, which can compensate a movement of 350 mm (Pos.7, FIG.2). Two additional tubes containing diagnostics cables, water circuits, pressurized air tubes, waveguides (Pos.4, FIG.2) and capacitor tuning rods are connected to the rear side of the capacitors. These volumes are evacuated down to 10^{-3} mbar and then filled with 50 mbar Ne. The use of Ne and monitoring of the pressure allow easy identification of vacuum leaks.
The RF power from the two generators is delivered to the straps through the matching-decoupling system via DC breaks [5] and two line RF transmission line stretchers (Pos. 11, FIG.2) to compensate for the radial movement of the antenna carrier. Gas puffing (H_2 or D_2) into the scape-off layer, foreseen to improve RF coupling conditions for non standard magnetic shapes, is accomplished using gas pipes with 1 mm diameter holes at both sides of the antenna head wall and connected with 6 mm diameter gas supply tubes. Two Piezo valves mounted at the rear side of the antenna box can deliver gas pulses equal to or longer than 10 ms. The gas flow can be adjusted by a pre-set pressure up to 10 bars.

4. Antenna diagnostics

At 8 positions in the graphite tiles along the circumference of the antenna head the temperature is measured by type K thermocouples. An additional four type K thermocouples are mounted in the center and capacitor side of the straps. Furthermore, resistive thermal sensors (RTS) Pt100 are mounted at the capacitor housings and at the rear side of the antenna box to monitor the heat load distribution. Each line is foreseen with RF current and voltage probes. Microwave reflectometers are foreseen to measure the electron density profile in front of the ICRH antenna head. One pair of horn antennas is mounted in the upper, and one in the lower part of the rear wall of the antenna head. Near the equatorial plane two groups of each 5 horn antennas are proposed for poloidal correlation spectrometry in the operational phase OP-2 of W7-X to measure turbulence characteristics of the plasma.

5. ICRH Operational Scenarios for fast ion generation and plasma heating in W7-X

The average magnetic field on the plasma axis of W7-X is $B_0 = 2.5$T, required for central plasma heating with 140 GHz electron cyclotron resonance heating (ECRH).
The bean-like plasma shape in front of the antenna in port AEE31, together with the contours of B are depicted in FIG. 3. For the nominal central field $B_0 = 2.5$T, the frequency band of the ICRH system in W7-X allows to deposit RF power to various ion species. As shown in FIG. 3a, Hydrogen, Deuterium and Helium-4 ions can be heated at the highest RF frequencies available f~37-38 MHz. Additionally, Helium-3 ions can be heated with ICRH at f~25-26 MHz (FIG. 3b).

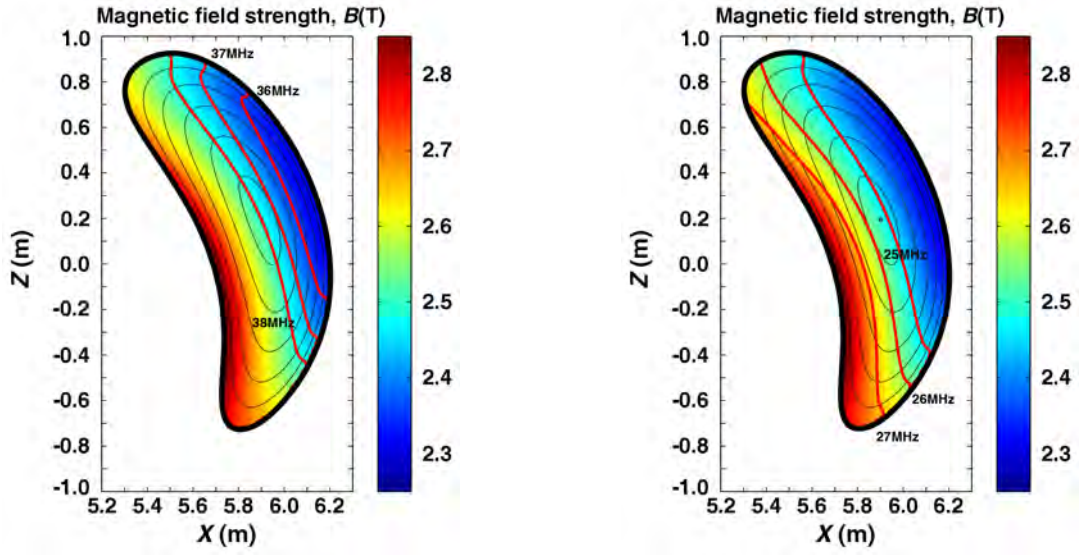

FIG. 3. Contour plot of the magnetic field strength for the standard configuration of W7-X in the plasma cross-section facing the ICRH antenna. Location of ion cyclotron resonance layers as a function of RF frequency: (a) H ($\omega = \omega_{ci}$) and D, ^{4}He ions ($\omega = 2\omega_{ci}$); (b) ^{3}He ions ($\omega = \omega_{ci}$).

Generating fast ions in W7-X at plasma densities below ~10^{20} m^{-3} can be achieved with the commonly used ICRH minority heating scenarios. However, this becomes significantly more challenging at very high plasma densities. Despite better absorptivity of RF waves at higher plasma densities, the tail energy of RF-heated minority ions decreases strongly with n_e. FIG. 4a shows an indicative example for the well-known scenario of H minority heating with $n_H/n_e = 3\%$ in D majority plasmas. The results have been computed with the SSFPQL code [9], and an average RF power density $\langle p_H \rangle = 1$ MW/m^3 absorbed by H ions has been assumed as input. Note that the average energy of RF-heated H ions scales as $(n_e)^{-2}$, in line with the scaling of the heating parameter ξ by Stix [10]. It is clear from FIG. 2(a) that because of the very high n_e (this implies high collisionality and reduced RF power per resonant ion), the tail formation for RF-heated H ions is highly inefficient. For example, at $n_e \sim 2\times10^{20}$ m^{-3} the average energy of the H ions is a mere 7.5 keV. The tail formation with RF heating can be made much more efficient by lowering the operational plasma density, e.g. for $n_{e0} \sim 7.5\times10^{19}$ m^{-3}, we find $\langle E_H \rangle \approx 64$ keV.

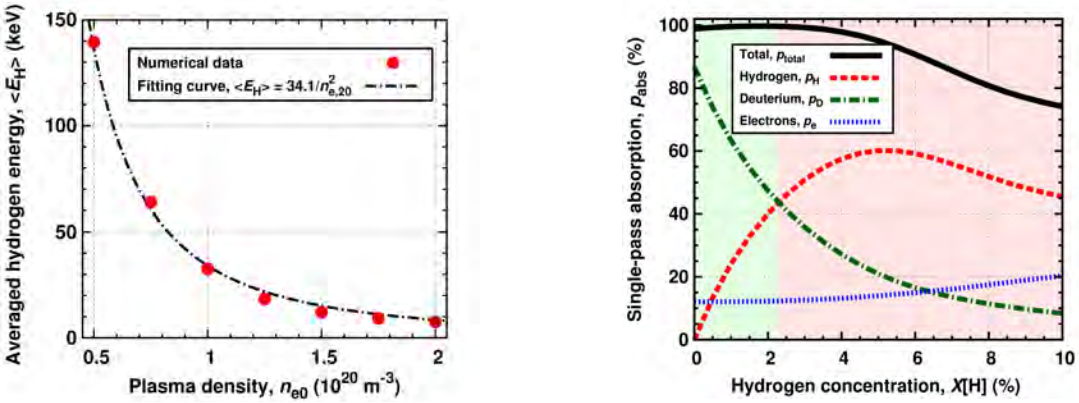

FIG. 4. (a) Average energy of RF-heated H minority ions, $n_H/n_e = 3\%$ in D majority plasmas as a function of the central plasma density. A power density absorbed by H ions $P_H = 1$ MW/m^3 is assumed as input in these calculations. (b) Estimated single-pass absorption by D, H and electrons as a function of H concentration at $f = 38$ MHz ($n_{e0} = 2\times10^{20}$ m^{-3}, $T_0 = 3$ keV).

There are essentially only 2 options to increase the energy of the H minority ions. At fixed background plasma density and temperature, the heating parameter by Stix scales as $\xi_{STIX} \sim P_{RF} / n_{mino}$, where P_{RF} is the RF power density absorbed by minority ions, which we assumed here as $P_{RF} = 1$ MW/m^3.

The first option for maximizing tail energies of H minority ions is to increase the RF power density. However, the amount of ICRH power that can be made available to W7-X using 1 RF port is limited ($P_{ICRH} \sim$ 1-2 MW), and reaching central RF power densities much higher than the considered value 1 MW/m^3 is likely to be difficult. At first sight, it is easier to follow the second option and decrease the concentration of H minority ions much below 3%.

FIG. 4b shows an estimation for the single-pass absorption (SPA) by H minority and D majority ions as a function of H concentration, computed with the TOMCAT code [11]. This code is based on tokamak geometry but for these calculations TOMCAT was modified ([12]), to include a proper treatment of the radial dependence of the stellarator magnetic field B. For the conditions considered, electrons also absorb between 10% and 20% of the launched RF power via the combined mechanisms of electron Landau damping and transit time magnetic pumping. As follows from FIG. 4b, the distribution of RF power between D and H ions depends strongly on the H concentration X[H]. Single-pass damping by H is maximized at X[H] ~ 5% ($p_{SPA} \sim 95\%$, $p_H \sim 60\%$, $p_D \sim 20\%$ and $p_e \sim 15\%$). However, if operating at plasma densities above 10^{20} m^{-3}, H concentrations of this level (a few %) are already too large for fast-ion tail creation in W7-X (see FIG. 4a).

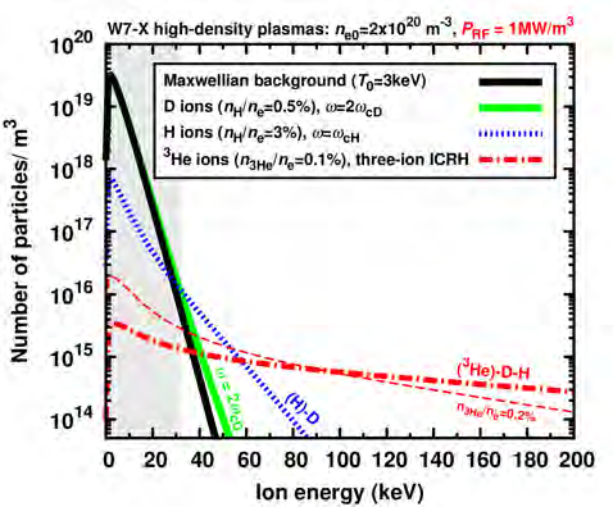

FIG. 5. Energy distribution functions of RF-heated ions in high-density plasmas of W7-X for the three ICRH scenarios of interest. Black line – Maxwellian background; blue dotted line – H minority heating with X[H] = 3%; green line – second harmonic D heating (X[H] = 0.5%); red line – three-ion minority heating of ^{3}He ions (X[^{3}He] = 0.1%) in H-D mixture. RF power density P_{RF} = 1MW/m^3 is chosen as input.

Lowering the H concentration to very low levels, e.g., X[H]=0.5%, would also not help to generate energetic H ions. As the calculations show, the residual H minority ions absorb only ~15% of the launched RF power, whereas the D (or ^{4}He) majority ions absorb most of the power (>70%) via second harmonic absorption ($2\omega_{cD} = \omega_{cH}$). This damping mechanism is a finite-Larmor-radius effect which improves with increasing ion beta β_i [13] and in high density W7-X plasmas becomes very efficient.

A far more interesting option is heating a small population of ^{3}He ions in H-D or H-^{4}He plasma mixtures with $n_H/n_e \sim 70\%$. This has been recently verified experimentally on both C-Mod and JET [3,4]. This scenario is one of the so-called three-ion ICRH scenarios, which allow an effective RF power absorption at very low concentrations of minority ions (~ 1% and even below) (see also [2]). The high absorptivity of RF power at very low minority concentrations is achieved by adjusting the concentration of the two majority ion species (e.g., H and D) to maximize the left-hand polarized RF component E_+ in the region of the cyclotron resonance of a third minority (e.g. ^{3}He) species. Furthermore, in contrast to H minority heating in D majority plasmas, the

cyclotron resonance of ^{3}He minority ions does not have any degeneracy with the second harmonic ion cyclotron resonances of the majority ions.

As can be clearly seen in FIG. 5, this scenario can produce a significantly larger number of energetic ions compared to what can be obtained from H minority and second harmonic D heating (see FIG. 5). For $P_{RF} = 1$ MW/m^3 (the same input power density for all ICRH scenarios of interest), the number of fast ions with energies $E_i > 50$ keV produced by three-ion ^{3}He heating ($X[^3He] = 0.1\%$) is 6 times larger than for H minority heating (X[H] = 3%), resp. $1.1\text{x}10^{17}$ m^{-3} vs. $1.9\text{x}10^{16}$ m^{-3}, respectively. This comparison becomes even more impressive when comparing the number of ions with $E_i > 100$ keV. While H minority heating yields only $n_{fast} = 9.2\text{x}10^{13}$ m^{-3}, the three-ion ^{3}He heating is about ~800 times more efficient in this energy range, $n_{fast} = 7.2\text{x}10^{16}$ m^{-3}.

6. Ion Cyclotron Wall Conditioning for W7-X

With the permanent magnetic field of W7-X, use of the ICRH system is also planned for Ion Cyclotron Wall Conditioning (ICWC). The coupling of RF power to create plasma is not limited to cyclotron resonance layers. Via collisional absorption homogeneous discharges can be created extending into the SOL which ensures an optimal plasma wetted wall area. The conditioning procedure consists of series of short ICRF pulses (2-5 s) with a duty cycle of 5 to 20%. The wall released hydrogen and impurities are efficiently evacuated in the interval between subsequent ICRF pulses.

7. Conclusions

An ICRH system for W7-X is under construction in a collaborative effort between IEK-4, Forschungszentrum Jülich and LPP/ERM-KMS, Brussels, for implementation in W7-X starting from experimental campaign OP1.2b. It is designed to couple up to ~2MW of ICRH power for frequencies in the range 25-38MHz. Various ICRH heating schemes for plasma heating and the creation of fast particle populations have been identified. The three-ion heating scheme uses a low concentration (< 1%) of a minority ion (e.g. ^{3}He, f = 25MHz) in a plasma consisting of two majority ions (H and D). This allows to substantially increase the amount of absorbed RF power per resonant ion, and accelerate ^{3}He minority ions to energies between 50 and 100 keV or higher, even at the highest plasma densities. In addition, H minority or second harmonic D majority absorption can be used for efficient plasma heating. E.g. at $n_e > 2\times10^{20}$ m^{-3}, H minority ions dominantly absorb RF power if $n_H/n_e > 2$–3%. Furthermore, at lower H concentration, $n_H/n_e < 2\%$, second harmonic heating of D ions becomes the dominant power absorption channel. Finally, the antenna will is also ideally suited for Ion Cyclotron Wall Conditioning of W7-X in presence of the permanent magnetic field.

8. References

[1] BOSCH, H.-S. et al., Nucl. Fusion 53, 126001 (2013)

[2] KAZAKOV, Ye.O. et al., Nucl. Fusion 55, 032001 (2015)

[3] KAZAKOV, Ye.O. et al., “Plasma heating and generation of energetic ions with novel three-ion ICRF scenarios on Alcator C-Mod and JET tokamak facilities”, Invited Talk at the 58th Annual Meeting of the APS Division of Plasma Physics (31 Oct – 4 Nov, 2016, San Jose, California, USA).

[4] WRIGHT, J., WUKITCH, S. et al., this conference, "Experimental results from three-ion species heating scenario on Alcator C-Mod", Paper EX/P3

[5] ONGENA, J., MESSIAEN, A.M., et al., Physics of Plasmas, 21, 061514 (2014).

[6] ONGENA, J., MESSIAEN, A.M., et al., 25th Fusion Energy Conference (FEC 2014)

(13 -18 October 2014, Saint Petersburg, Russia), Paper TH/P6-60

[7] SCHWEER, B., ONGENA, J., BORSUK, V. et al., 29th Symposium on Fusion Technology (SOFT), (5-9 September 2016, Prague, Czech Republic), Paper P1.34; submitted to Fusion Engineering and Design.

[8] DUWE, R., KÜHNLEIN, W, MÜNSTERMANN, H., Fusion Technology 355–358 (1994)

[9] BRAMBILLA, M. and BILATO, R., Nucl. Fusion 49, 085004 (2009)

[10] STIX, T.H., Nucl. Fusion 15, 737-754 (1975)

[11] VAN EESTER, D. and KOCH, R. Plasma Phys. Control. Fusion 40, 1949-1975 (1998).

[12] KAZAKOV, Ye.O., VAN EESTER, D, ONGENA, J., and FÜLÖP, T., AIP Conf. Proc. 1580, 342-345 (2014).

[13] PORKOLAB, M., BÉCOULET, A., et al., Plasma Phys. Control. Fusion 40, A35-A52 (1998).

9. Acknowledgements

This work has been carried out within the framework of the EUROfusion Consortium a nd has received funding from the EURATOM research and training programme 2014-2018 under grant agreement No 633053. The views and opinions expressed herein do not necessarily reflect those of the European Commission.